ChemComm

Accepted Manuscript

ROYAL SOCIETY OF CHEMISTRY

rsc.li/chemcomm

ChemComm

View Article Online
DOI: 10.1039/C7CC01007A

COMMUNICATION

Specific and relative detection of urinary microRNAs signature in bladder cancer for point-of-care diagnostics

Received 00th January 20xx,
Accepted 00th January 20xx

DOI: 10.1039/x0xx00000x

www.rsc.org/

Nan Cheng,[a] Yuancong Xu[a], Yunbo Luo[a,b], Liye Zhu[a], Yitong Zhang[c], Kunlun Huang[a,b] and Wentao Xu[a,b *]

We present a dual-isothermal cascade strategy assisted by a lateral flow peptide nucleic acid biosensor for point-of-care detection of urinary microRNAs without a temperature protocol and complex instruments. The assay is expected to be of great promise for bladder cancer diagnosis and point-of-care.

MicroRNAs are a class of endogenous, non-protein coding small RNA molecules (17-25 nucleotides) that act as gene-expression regulators and play important roles in numerous biological processes.[1] Recent findings indicate that the presence of microRNAs in urine may provide a valuable source of stable and noninvasive biomarkers in bladder cancer.[2, 3] Accordingly, point-of-care biosensing platforms for urinary microRNA detection are urgently needed to indicate cancer stage and response to treatment.

Among the currently available and common techniques for microRNA detection, exponential isothermal amplification (EXPAR) is an advanced isothermal amplification strategy that can generate thousands of single-strand DNA (ssDNA) at a constant temperature.[4] It has been successfully applied in the detection of microRNA as a powerful signal amplification tool to derive various sensors, such as liquid colorimetric biosensors,[5] fluorescent biosensors,[6, 7] electrochemical biosensors,[8, 9] and surface-enhanced Raman spectroscopy (SERS).[10] However, these techniques are still challenged with high background and nonspecific amplification due to their small size and especially high similarity of sequences among family members.[11, 12] More importantly, these biosensing platforms are limited by absolute quantification of microRNAs, leading to results that may significantly vary depending on the method used, resulting in a still unmet challenge at the point-of-care.[13] In fact, relative changes in the expression of target microRNAs compared to an internal reference have practical significance for cancer diagnoses.[13-17] Therefore, strategies with high specificity and relative quantification for urinary microRNAs detection are urgently needed at the point-of-care.

Here, we introduce a dual isothermal cascade strategy (base stacking hybridization and exponential isothermal amplification, BSH-EXPAR) assisted by a trident-like lateral flow peptide nucleic acid biosensor (TLPB) to overcome these limitations. The system features the following three main components. (A) BSH-EXPAR. BSH is a high specific phenomenon that has been used to describe the additional stability associated with hybridization reactions wherein two oligonucleotides hybridize in a contiguous tandem to a longer complementary DNA single strand.[18] After base design optimization, this technique is typically used for single-base discrimination.[19] Introducing BSH to EXPAR and optimizing the isothermal process can effectively overcome poor specificity. (B) Peptide nucleic acid (PNA) probe. The PNA probe allows high selectivity for the target with very low background due to advantages of PNA itself such as increased sequence specificity, high binding affinity, its superior stability to complementary DNA, and its powerful discrimination for single-base mismatched DNA.[20-22] To consistently enhance specificity, we introduced PNA instead of DNA as a probe for the lateral flow biosensor for the first time. (C) Trident-like lateral flow biosensor. We first reported this biosensor for the qualitative detection of stacked genetically modified soybeans after careful consideration of cross-reactivity and the limitations of Washburn's theory.[23] Here, this is the first application of the biosensor for relative quantitative detection.

The assay strategy is illustrated in Scheme 1. Urinary microRNA was viewed as a target and applied in the BSH-EXPAR solution, which consists of a microRNA-specific primer, a universal primer, Bst. polymerase, Nt.BstNBI, deoxyribonucleotide triphosphates (dNTPs), and buffer. As shown in **Scheme 1A**, the universal primer involves four regions (green, brown, red and blue), and sequences of the green region are complementary to the microRNA-specific primer partly at its 3' ends. Therefore, an EXPAR process occurs efficiently in the presence of target microRNA based on the phenomenon of BSH. The target microRNA (red) can hybridize with the 5' ends of the microRNA-specific primer (step 1). Then, the microRNA-specific primer extends along the universal primer in the presence of Bst polymerase and dNTPs to form stable double-stranded DNA duplexes with a cleavage site (brown) for nicking enzyme Nt.BstNBI (step 2). The cleavage (step 3) can generate a short single-stranded DNA (ssDNA), which consists of a universal linker (blue) and a DNA sequence with the same sequence as target microRNA (red), except for the change of U to T (step 4).The ssDNA can act as a new primer to initiate other amplifications (step 5). Thus, the extension (step 6) and cleavage (step 7) can be repeated

[a] Beijing Advanced Innovation Center for Food Nutrition and Human Health, College of Food Science & Nutritional Engineering, China Agricultural University, Beijing 100083, China
[b] Beijing Laboratory for Food Quality and Safety, College of Food Science and Nutritional Engineering, China Agricultural University, Beijing 100083, China.
[c] Ocean college, Zhejiang University of Technology, Hangzhou 310014, China
† Electronic Supplementary Information (ESI) available.
See DOI: 10.1039/x0xx00000x

continuously and result in an exponential amplification. Finally, a large amount of ssDNA (blue and red) can be produced (step 8), and theoretical analysis from 1 target input to 2^{n-1} product output is presented in Table S1.

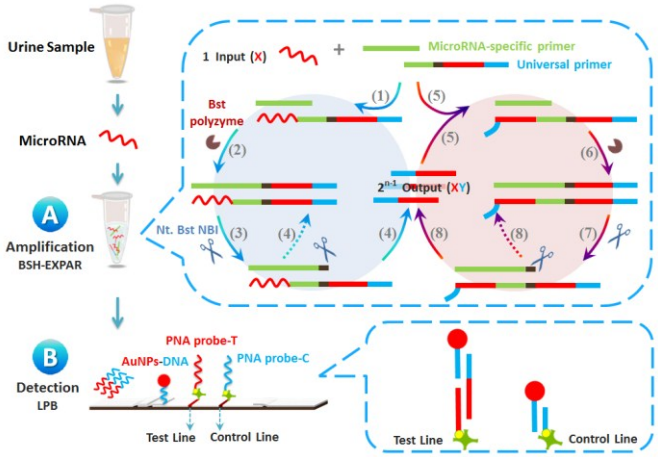

Scheme 1. Schematic illustration of the base stacking hybridization and exponential isothermal amplification and lateral flow peptide nucleic acid biosensor. (A) Amplification by BSH-EXPAR; (B) Detection amplified products by FPB.

The visual detection of single amplified products was performed on the lateral flow peptide nucleic acid biosensor (LPB), and a typical hybridization principle is shown in **Scheme 1B**. The AuNPs-DNA conjugate was first dispensed on the conjugate pad, and two biotinylated PNA probes (T and C) were pre-immobilized on the nitrocellulose membrane through a biotin-streptavidin interaction to form the test and control lines, respectively. The sample solution containing amplified ssDNA was applied on the sample pad. The solution was driven by capillary flow, passed the conjugate pad, and then rehydrated the AuNPs-DNA conjugates. The blue region of the ssDNA hybridized with the DNA probe of the AuNPs-DNA conjugates. The as-formed hybrid continued to migrate along the biosensor and was captured on the test line through the reaction between the red region of ssDNA and the PNA probe-T. The accumulation of AuNPs-DNA conjugates on the test line produced a characteristic red line. Excess AuNPs-DNA conjugates continued to migrate through the control line and were captured by the PNA probe-C, thus forming the second red line on the control line and indicating that the biosensor worked properly.

The principle of expanding multiplex and relative detection was illustrated in **Scheme 2**. It should be noted that different microRNAs (X_1, X_2, X_3) can be converted to the BSH-EXPAR products (YX_1, YX_2, YX_3) with the same linker (Y, blue region), which can be detected with the same DNA capture probe of the AuNPs-DNA conjugates, the same PNA probe-C on control line and the specific PNA probe-T. Together, they can simply and effectively form specific sandwich-like hybridizations for multiplexed microRNA (X_1, X_2, and X_3) detection using TLPB. The relative intensity (RI_1 or RI_2) is defined as the peak area of the test lines for X_1 or X_2 divided by the peak area of the test line of X_3 of each individual biosensor. Therefore, the different RIs reflected the various relative expression level for the targets (X_1 and X_2) by means of comparing the internal reference (X_3), indicating that the developed sensing system can relatively quantify multi-microRNAs.

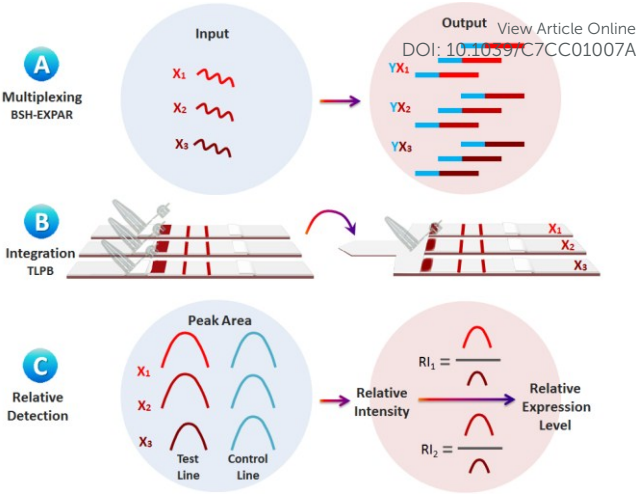

Scheme 2. Schematic illustration of multiplex and relative detection of microRNAs. (A) Multiplex BSH-EXPAR (Input: X_1, X_2, X_3; Output: YX_1, YX_2, YX_3); (B) Detecting multiple amplified products by TFPB; (C) Relative detection of the peak area of test lines for X_1 or X_2 divided by the peak area of test line for X_3 (RI_1 or RI_2).

For the proof-of-concept experiment, we selected microRNA 126 and microRNA 182 (code X_1 and X_2) as our initial targets (Table S2); they were robust since all samples contained readily detectable amounts of these species and were typically used to distinguish bladder cancer patients from controls.[2, 24, 25] In addition, microRNA 152 (code X_3) was considered a suitable reference gene for analyzing circulating microRNAs in the urine of bladder cancer patients.[2] The BSH-EXPAR amplification process was verified via agarose gel electrophoresis (**Figure 1**). This strategy depended on microRNA-specific primers, universal primers, Bst. polymerase and Nt.BstNBI, as no target bands were observed when any of these were omitted from the reaction. The accuracy of this multiplex reaction was based on the approximately equal amplification efficiency of the primers, which was examined by real-time BSH-EXPAR. According to previous reports, when three primer sets were added to a reaction mixture, the reaction could efficiently amplify each target with levels reaching the detection limits in approximately the same time and with similar amplification efficiency. As shown in Figure S1, around the same amplification efficient was obtained with this design, indicating that the cascade was reliable and well-suited for simultaneous measurements.

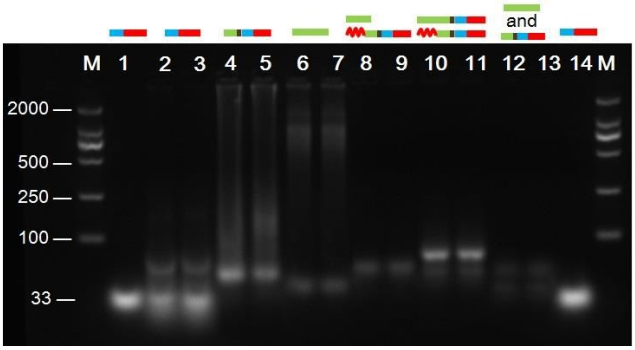

Figure 1. The agarose gel electrophoresis image of the BSH-EXPAR amplification process. Lane M: DL2000 DNA marker. Lanes 1 and 14: Synthetic product ssDNA (blue and red) as marker. Lanes 2 and 3: Positive control. Lanes 4 and 5: MicroRNA-specific primer omitted. Lanes 6 and 7: Universal primer omitted. Lanes 8 and 9: Bst. Polymerase omitted. Lanes 10 and 11: Nt.BstNBI omitted. Lanes 12 and 13: Negative control. The concentration of target microRNA was 1 nM.

We further employed agarose gel electrophoresis to investigate the effect of the stacking hybridization base number on the brightness of the target band (Figure S2). The results indicated that 5 stacking hybridization bases without blank signal was suitable for this design. Moreover, a reaction time of 20 min was chosen for BSH-EXPAR based on Figure S1. Additionally, we studied the effect of the amount of the AuNPs-DNA conjugation, the concentration of the PNA probe, and the hybridization time of DNA-PNA by comparing the analytical performances of TLPB (Figure S3). After optimization, 2.5 μL of AuNPs-DNA conjugation, 50 μM of the PNA probe, and 5 min of DNA-PNA hybridization were selected to be used in the following experiments.

Under the optimal conditions determined above, the selectivity of the proposed assays was examined using the interference microRNAs with one-base mismatch (1M), two-base mismatch (2M), and three-base mismatch (3M) of microRNA 126, microRNA 182, and microRNA 152 at the 5' end, at the 3' end, and in the middle. As shown in **Figure 2**, the peak area of targets scarcely changed compared with the blank control, while the response from the interfering microRNA remained as low as the blank control, with no notable cross-reactivity. The yellow dotted line represents the cutoff value for positive calls, which was set as the value of negative control plus three times the standard deviation (SD) of the negative control. The high hybridization selectivity of the cascade strategy was achieved by taking advantage of the base tracking effects of BSH and the binding specificity between targets and PNA probes of TLPB.

To evaluate the sensitivity, we examined the approach using different concentrations of target microRNAs (ranging from 0 to 1 nM). **Figure 3a** represents a typical image of TLPB. Visual detection for target microRNAs can be achieved by observing the color of the test lines, which can be observed as low as 1 fM. There is no colored band on the test line of the TLPBs in the absence of target microRNAs (negative control). Quantitative detections of X_1 were performed by recording the intensities of the test lines using a portable strip reader. The limit of detection (LOD) was calculated to be 0.6 fM based on negative control plus three times the SD of the negative control. The resulting plot of response versus microRNA concentrations was linear over the 1 fM to 100 pM range as shown in **Figure 3b**. Similar detection results for X_2 and X_3 were also obtained (data not shown). This detection at the femtomolar-level was suitable for independent quantitative work in urine.[24, 26] Obviously, our assay's sensitivity was superior to the recently reported lateral flow biosensors for microRNA detection (Table S3).

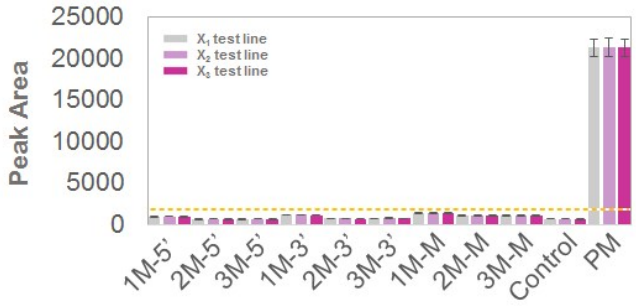

Figure 2. Specificity investigations of one-base mismatch (1M), two-base mismatch (2M), and three-base mismatch (3M) of microRNA 126, microRNA 182, and microRNA 152 at the 5' end, at the 3' end, and in the middle. The concentration of microRNAs was 1 pM. The yellow dotted line represents the value of negative control plus three times the standard deviation (SD) of the negative control and was used as the cutoff value for a positive signal.

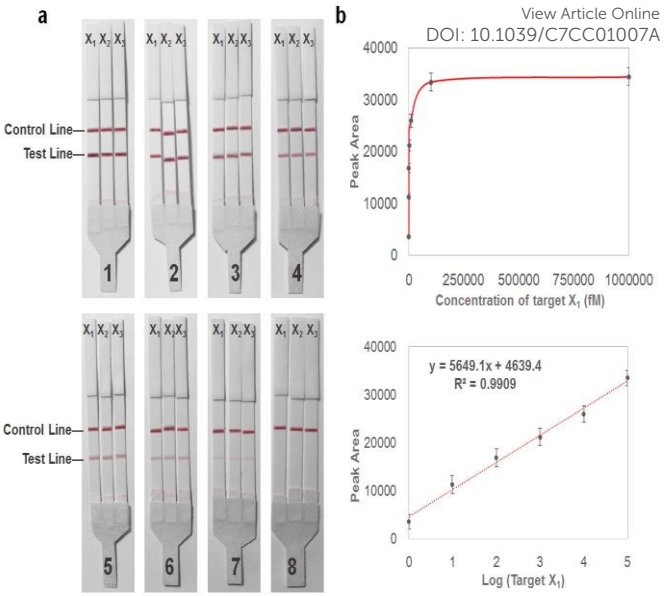

Figure 3. The performance of the BSH-EXPAR-TLPB cascade in response to various concentrations of target microRNA. (a) Typical photo images. Target concentrations: (1) 1 nM; (2) 100 pM; (3) 10 pM; (4) 1 pM; (5) 100 fM; (6) 10 fM; (7) 1 fM; (8) 0. (b) The calibration curve.

At the clinical level, microRNA analysis of species in urine sample revealed the ratios of microRNA 126: microRNA 152 (X_1:X_3) and microRNA 182: microRNA 152 (X_2:X_3), which showed an average 9.9-fold and 3.9-fold increase in urine samples of patients with bladder cancer patients in comparison to healthy donors.[2] Therefore, we tried to detect different ratios of targets (X_1 or X_2) and their markers (X_3) at basal concentrations of 1 fM, which was selected according to previous reports that quantified microRNA in urine.[24, 26] **Figure 4a** displays the bar graph of TLPB's peak area using increased ratios of 1-fold, 5-fold, 10-fold, 15-fold, and 20-fold of X_1:X_3 and X_2:X_3, and **Figure 4b** shows the relationship between RI_1 and the logarithm of ratios of X_1:X_3. Similar results of RI_2 versus X_2:X_3 were also obtained (data not shown), indicating that the proposed assays were reasonable for the quantitative work of relative expression measurements.

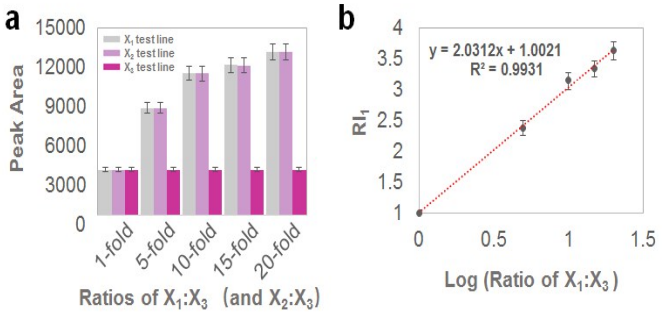

Figure 4. The performance of TLPBs in response to various ratios of targets (X_1 or X_2) and their markers (X_3) at basal concentrations of 1 fM. (a) Bar graph of TLPB's peak areas with the increased ratios of 1-fold, 5-fold, 10-fold, 15-fold, and 20-fold of X_1:X_3 and X_2:X_3. (b) The calibration curve of relative intensities versus logarithm of ratios of X_1:X_3.

To demonstrate the capability of the developed method for microRNA detection in complex biological samples, microRNA 126, microRNA 182 and microRNA 152 extracted from urine samples of bladder cancer patients and healthy donors were analyzed using the BSH-EXPAR cascade. As shown in Fig. S5 (A-C), the relative data obtained by using the developed method were consistent with results obtained using the quantitative real-time polymerase chain reaction (qRT-PCR), indicating that the proposed method was capable of microRNA quantification in real complex samples. In addition, it was observed that the microRNA 126 and microRNA 182 showed higher expression levels in bladder cancer patients compared with healthy donors (Fig. S5D), which was in good agreement with previous reports.[24-28] The matrix effect of the method was investigated for the detection of recoveries in the urine with added microRNA 126 at given concentrations. The estimated recoveries of BSH-EXPAR range from 93.41% to 104.38% (Table S4), which indicated the high capability of the proposed method for sensitive microRNA detection in real complex samples.

In summary, the developed assay quantified the absolute amount of microRNAs down to 0.6 fM and a 20-fold relative expression of the target, which was reasonable and suitable for quantitative work in urine samples. Moreover, it combined BSH with EXPAR amplification in one system and introduced PNA as an alternative probe into lateral flow biosensors, which greatly improved specificity for differentiating one-base mismatches. In addition, targets were detected in urine samples without temperature protocols and sophisticated instruments, making it possible to use them as non-invasive biomarkers in cancer detection and as predictors of therapeutic responses at the point-of-care. Alternatively, integrated devices based on this design could be envisaged by simply changing the reaction solution for amplification into a freeze-dried powder and using pre-coated tubes.

Acknowledgments

This work was financially supported by the Natural Science Foundation of China (Grant No.31671922).

Notes and references

1. M. Zorc and T. Kunej, *MicroRNA*, 2015, **4**, 205-208.
2. M. Hanke, K. Hoefig, H. Merz, A. C. Feller, I. Kausch, D. Jocham, J. M. Warnecke and G. Sczakiel, in *Urologic Oncology: Seminars and Original Investigations*, Elsevier, 2010, pp. 655-661.
3. T. Ichimi, H. Enokida, Y. Okuno, R. Kunimoto, T. Chiyomaru, K. Kawamoto, K. Kawahara, K. Toki, K. Kawakami and K. Nishiyama, *International journal of cancer*, 2009, **125**, 345-352.
4. H. Jia, Z. Li, C. Liu and Y. Cheng, *Angewandte Chemie International Edition*, 2010, **49**, 5498-5501.
5. Y. Zhang, J. Hu and C.-y. Zhang, *Analytical chemistry*, 2012, **84**, 9544-9549.
6. W. Li, T. Hou, M. Wu and F. Li, *Talanta*, 2016, **148**, 116-121.
7. K. Wang, K. Zhang, Z. Lv, X. Zhu, L. Zhu and F. Zhou, *Biosensors and Bioelectronics*, 2014, **57**, 91-95.
8. Y. Yan, D. Zhao, T. Yuan, J. Hu, D. Zhang, W. Cheng, W. Zhang and S. Ding, *Electroanalysis*, 2013, **25**, 2354-2359.
9. Y. Yu, Z. Chen, L. Shi, F. Yang, J. Pan, B. Zhang and D. Sun, *Analytical chemistry*, 2014, **86**, 8200-8205.
10. L.-P. Ye, J. Hu, L. Liang and C.-y. Zhang, *Chemical Communications*, 2014, **50**, 11883-11886.
11. H. Zhang, F. Li, B. Dever, X.-F. Li and X. C. Le, *Chemical reviews*, 2012, **113**, 2812-2841.
12. X. Zhou, Y. Liang, Y. Xu, X. Lin, J. Chen, Y. Ma, L. Zhang, D. Chen, F. Song and Z. Dai, *Biosensors and Bioelectronics*, 2016, **80**, 378-384.
13. F. Degliangeli, P. Kshirsagar, V. Brunetti, P. P. Pompa and R. Fiammengo, *Journal of the American Chemical Society*, 2014, **136**, 2264-2267.
14. A. Szafranska, T. Davison, J. John, T. Cannon, B. Sipos, A. Maghnouj, E. Labourier and S. Hahn, *Oncogene*, 2007, **26**, 4442-4452.
15. O. Slaby, M. Svoboda, P. Fabian, T. Smerdova, D. Knoflickova, M. Bednarikova, R. Nenutil and R. Vyzula, *Oncology*, 2008, **72**, 397-402.
16. M. Saul, C. Zhao, T. Driessen, B. Eisinger and S. Gammie, *Neuroscience*, 2016, **312**, 130-140.
17. T. Nara, S. Narita, H. Mingguo, T. Yoshioka, A. Koizumi, K. Numakura, H. Tsuruta, A. Maeno, M. Saito and T. Inoue, *Carcinogenesis*, 2016, **37**, 1129-1137.
18. Z. Lu, D. Duan, R. Cao, L. Zhang, K. Zheng and J. Li, *Chemical Communications*, 2011, **47**, 7452-7454.
19. D. Duan, K.-x. Zheng, Y. Shen, R. Cao, L. Jiang, Z. Lu, X. Yan and J. Li, *Nucleic acids research*, 2011, **39**, e154-e154.
20. S.-R. Ryoo, J. Lee, J. Yeo, H.-K. Na, Y.-K. Kim, H. Jang, J. H. Lee, S. W. Han, Y. Lee and V. N. Kim, *ACS nano*, 2013, **7**, 5882-5891.
21. T. Sato, Y. Sato and S. Nishizawa, *Journal of the American Chemical Society*, 2016, **138**, 9397-9400.
22. X. Xia, X. Piao and D. Bong, *Journal of the American Chemical Society*, 2014, **136**, 7265-7268.
23. N. Cheng, Y. Shang, Y. Xu, L. Zhang, Y. Luo, K. Huang and W. Xu, *Biosensors and Bioelectronics*, 2017, **91**, 408-416.
24. J. A. Weber, D. H. Baxter, S. Zhang, D. Y. Huang, K. H. Huang, M. J. Lee, D. J. Galas and K. Wang, *Clinical chemistry*, 2010, **56**, 1733-1741.
25. L. Liu, S. Jiang, L. Wang, Z. Zhang and G. Xie, *Microchimica Acta*, 2015, **182**, 77-84.
26. I. Z. Ben-Dov, Y.-C. Tan, P. Morozov, P. D. Wilson, H. Rennert, J. D. Blumenfeld and T. Tuschl, *PloS one*, 2014, **9**, e86856.
27. M. Z. Mousavi, H.-Y. Chen, K.-L. Lee, H. Lin, H.-H. Chen, Y.-F. Lin, C.-S. Wong, H. F. Li, P.-K. Wei and J.-Y. Cheng, *Analyst*, 2015, **140**, 4097-4104.
28. X. Min, Y. Zhuang, Z. Zhang, Y. Jia, A. Hakeem, F. Zheng, Y. Cheng, B. Z. Tang, X. Lou and F. Xia, *ACS applied materials & interfaces*, 2015, **7**, 16813-16818.